NORSAR

NORSAR Scientific Report No. 1-2000/2001

Semiannual Technical Summary

1 April - 30 September 2000

Frode Ringdal (ed.)

Kjeller, November 2000

6.4 Synthetic travel times for regional crustal transects across the Barents Sea and the adjacent western continental margin

Introduction

The CTBT monitoring tasks have created a renewed interest for more precise estimation of local and regional travel times through a laterally varying lithosphere.

The crustal and seismic velocity structure of the Barents Sea varies significantly (Faleide, 2000):

- The thickness of the sedimentary cover varies from 0 to 20 km
- The depth to Moho varies from 20 to 45 km
- The thickness of crystalline crust varies from 10 to 45 km

If we include the western Barents Sea-Svalbard continental margin and the adjacent Norwegian-Greenland Sea, Moho rises to depths of 8 - 10 km and the thickness of the oceanic crystalline crust is typically 5 - 7 km.

The crustal heterogeneity of the Barents Sea region affects the accuracy of any seismic event location. Locating seismic events in this area with the 1D Barents Sea crustal model (Kremenetskaya and Asming, 1999) will give a location which will vary significantly in quality, depending on azimuth and distance between the seismic array (e.g. SPITS) and the earthquake (Schweitzer, 2000). The 1D Barents Sea crustal model is already known as an improvement with respect to the standard Earth model IASP91 (Kennett and Engdahl, 1991), as used at the IDC. It has a thicker crust (40 instead of 35 km), 6.9 (and 3.1)% higher P velocities in the two layered crust, and slightly higher velocities below the Moho.

In this report, we have calculated synthetic travel times for the first arrivals along four regional crustal transects across the Barents Sea and the adjacent western continental margin (Faleide, 2000) (Fig. 6.4.1) and compared these with the corresponding travel times predicted by the Barents Sea regional velocity model of Kremenetskaya and Asming (1999) which today is used to localize earthquakes in this area. Comparing these travel time curves can give some indication of how large the uncertainties tied to the localization of earthquakes with the Barents Sea model are.

Along one of the transects, between the spreading axis in the Greenland Sea and SPITS on Svalbard (Fig. 6.4.1), we have also carried out a sensitivity study where we tested the travel time effects caused by variations in the Moho topography.

Western Svalbard margin

Transect 4, across the western Svalbard margin, is the most extreme with respect to a laterally varying crustal configuration (Fig. 6.4.2). The transect is 300 km long beginning east of SPITS and heading almost directly westwards to the Knipovich Ridge (Eiken *et al.*, 1994) (Fig. 6.4.1), which is a part of the Mid-Atlantic spreading ridge system. The model consists of the main sedimentary sequences and the oceanic and continental crystalline crust separated from the mantle by the Moho discontinuity. Each unit has been assigned a velocity within the velocity ranges given by Faleide (2000) (Fig. 6.4.2).

The Moho depth is varying from 10 km under the oceanic crust to 32 - 37 km under Spitsbergen (Fig. 6.4.2). The Moho configuration is thought to be well constrained by deep seismic reflection and refraction data along the transect, however, several sensitivity tests have been performed to reveal the importance of this structure. The sediment basins are up to 10 - 12 km deep but have minor influence on the travel times for events located around the spreading ridge. On the other hand there is a high-velocity layer consisting of carbonates (V ~ 6.2 km/s) located from distance 175 km to the eastern end of the transect. This layer is always carrying the first arrivals from offsets less than ~ 70 km.

A finite difference (FD) method (Podvin & Lecomte, 1991) as implemented in the NORSAR-2D software package was used to calculate the first arrivals including head waves which are usually not included in ray tracing techniques. This method gives the theoretical first arrivals but no information about later phases, amplitudes, or other ray attributes. It should therefore be kept in mind that for larger distances the first arrivals might not always carry enough energy to be detected at a seismological station. The ray paths for the first arrivals (both from the mantle and from the crust) are shown in Fig. 6.4.3.

Because the Moho topography is the most important feature affecting the travel times and ray paths at greater distances, this has been varied in a sensitivity test with five different models (Fig. 6.4.4). The different travel time curves constructed from each model are plotted in Fig. 6.4.5. For comparison the travel time curve from the regional Barents Sea model (Kremenetskaya and Asming, 1999) is also shown. The five different tests include:

1. The Moho depth was gradually decreased from 10 km to about 7.5 km towards the Knipovich Ridge.
2. The Moho depth was gradually decreased from about 17 to 13 km between distance 50 and 110 km.
3. The Moho depth was gradually increased from about 16 to 20 km between distance 75 and 150 km.
4. The depression in the Moho topography at distance 160 km was removed, resulting in a flat and shallower Moho below the continental crust.
5. The depression in the Moho was extended to the end of the profile resulting in a flat and deeper Moho below the continental crust.

It turned out that all the different modifications of the Moho geometry only had minor influence on the travel times (Fig. 6.4.5). On the other hand, the synthetic travel time curves are quite different from that based on the Barents Sea regional velocity model of Kremenetskaya and Asming (1999). Compared to the model based on Transect 4, the Barents Sea regional model are too fast up to about 200 km but slower at offsets larger than 200 km, an effect already observed by Schweitzer (2000).

Barents Sea

Three regional profiles across the Barents Sea (Fig. 6.4.1) (Faleide, 2000), each 1100 km long, have also been modelled. In Transect 1 the source was placed at ARCES (Δ = 100 km) resulting in wave propagation from ARCES to Novaya Zemlya. In Transect 2 the source was placed at SPITS (Δ = 50 km) resulting in wave propagation from SPITS to Novaya Zemlya. Two different tests were performed on Transect 3 between northern Norway and SPITS because there is a seismic station which need to be calibrated at both ends. By reversing the survey configura-

tion (source at SPITS instead of northern Norway) the crust will be sampled in a different way, creating a different travel time curve. However, the travel times at the end of the profiles will be the same because of the principle of reciprocity.

All the layers in Transects 1 - 3 (Fig. 6.4.6 - Fig. 6.4.9) including the crystalline crust and the mantle have been assigned a gradient based on the velocity ranges given by Faleide (2000). The velocities in the sediment basins vary from 4.0 or 4.5 km/s at top to 5.0 or 5.5 km/s at the bottom (depending on which transect, usually around 15 - 20 km depth). The crystalline basement has been assigned a gradient which gives a velocity of 6.0 or 6.2 km/s at zero depth and 6.8 or 6.9 km/s at about 30 - 40 km depth. The mantle has been assigned a velocity of 8.05 km/s at 25 - 30 km depth and 8.15 km/s at 70 km depth.

Fig. 6.4.6 and Fig. 6.4.7 show the different ray paths for the theoretical first arrivals for Transects 1 and 2, and Fig. 6.4.8 and Fig. 6.4.9 show the same for the two reversed models based on Transect 3. The different travel time curves based on these ray paths are shown in Fig. 6.4.10 together with that of Transect 4 and the regional Barents Sea crustal model.

Comparing the travel time curves at various offsets (Fig. 6), three different domains can be established:

- Δ = 0 - 180 km: The Barents sea crustal model is faster compared to all the other models. The difference is greatest for Transect 3 (3.5 s at offset 100 km) and smallest for Transect 1, which is almost identical with the Barents Sea crustal model up to 200 km.
- Δ = 180 - 450 km: At about 200 km the first arrivals from the Barents Sea crustal model are coming from the third layer (Vp = 8.10 km/s), as can be seen from the slope of the curve. Transect 1 and Transect 3 are slower (~ 0.8 s) and Transect 2 and 3 (reversed) are faster (~ 0.3 - 0.5 s).
- Δ = 450 - 1100 km: The crossover distance between the Barents Sea crustal model and Transect 2, 3, and 3 reversed can be seen at an offset of 550 - 600 km. Up to this point the Barents Sea crustal model seems to represent a good average velocity compared to the different transects, but beyond 450 km where the first arrivals are coming from the fourth layer in the Barents Sea crustal model (Vp = 8.23 km/s) this velocity is relatively high with respect to the other models, as it can be seen from the slope of the curve. The average slope of the three different travel time curves above an offset of 700 km is almost identical with the slope for the Barents Sea crustal model, which indicate almost the same velocity at 50 - 70 km depth. However, the differences in the total travel times are up to two seconds.

Discussion

Depending on the offset, travel time differences of up to 2 - 3 seconds are found when comparing travel time curves from the four transects to the standard 1D model (Barents Sea crustal model). This reveals that the Barents Sea crustal model needs to be refined in order to fit the velocity structure established along the regional transects. Because most of the observed events in this region are only observable at regional distances, it will be particularly important within this context to address upper mantle velocities, as a basis for Pn travel times.

The discrepancies between the different models in the first P-onset times of up to several seconds can easily lead to systematic epicenter differences of several tens of kilometers whenever the azimuthal coverage with observing stations is low. If the azimuthal coverage is good, the actual location may be calculated quite well but we will get larger observed travel time

residuals, especially for more nearby stations. The residuals again are the base for all estimations of epicentral error ellipses. That means, unusual high residuals will generally result in lower quality locations.

This modelling is based on deep seismic reflection and refraction data observed during the last decades and is providing no explicit information about the corresponding S-velocities in this region. As long as the Vp-to-Vs ratio is constant, single array locations are mostly influenced by this ratio because they use the S-P travel-time differences as a means for estimating epicentral distance. If the Vp-to-Vs ratio is not constant, the systematic errors due to the usage of incorrect models are even more difficult to evaluate. However, especially for smaller events the usage of S onsets is essential to get a hypocentral solution. A better knowledge of S velocities is therefore needed for a successful calibration of the European Arctic.

These results show that 2D and 3D modelling of travel times for the European Arctic are both feasible and desirable, aiming at producing source-site specific corrections as used and needed by IDC/CTBTO.

As further work we plan to continue the search for ground-truth events in the European Arctic in order to obtain more and better P-phase travel time observations for the whole region. The S-phase travel times should be addressed later, building in part on the improved P-phase based locations. Tomographic studies for the whole region based on surface waves and body wave data supplemented by receiver-function studies will also be potentially useful in a further delineation of lithospheric structure for the European Arctic.

J. I. Faleide
J. Schweitzer
H. Bungum
E. Møllegaard

References

Eiken, O., editor (1994): Seismic atlas of western Svalbard - a selection of regional seismic transects. Norsk Polarinstitutt Oslo, *Meddelelser* **130**, 73 pp. and 14 enclosures.

Faleide, J. I. (2000): Crustal structure of the Barents Sea - important constraints for regional seismic velocity and travel-time models. *Semiannual Technical Report 1 October 1999 - 31 March 2000. NORSAR Sci. Report* **2-1999/2000**, Kjeller, Norway, 119-129.

Kennett, B. L. N., and E. R. Engdahl (1991): Travel times for global earthquake location and phase identification, *Geophys. J. Int.* **105**, 429-466.

Kremenetskaya, E. and V. Asming (1999): Location calibration of the Barents region. In: Workshop on IMS location calibration, IDC technical experts group on seismic event location, Oslo, 12 - 14 January 1999, Technical Documentation.

Podvin, P. and I. Lecomte (1991): Finite difference computation of traveltimes in very contrasted velocity models: a massively parallel approach and its associated tools. *Geophys. J. Int.* **105**, 271-284.

Schweitzer, J. (2000): Recent profiling experiments in the Spitsbergen area - calibration data for the SPITS array. *Semiannual Technical Report 1 October 1999 - 31 March 2000. NORSAR Sci. Report* **2-1999/2000**, Kjeller, Norway, 93-105.

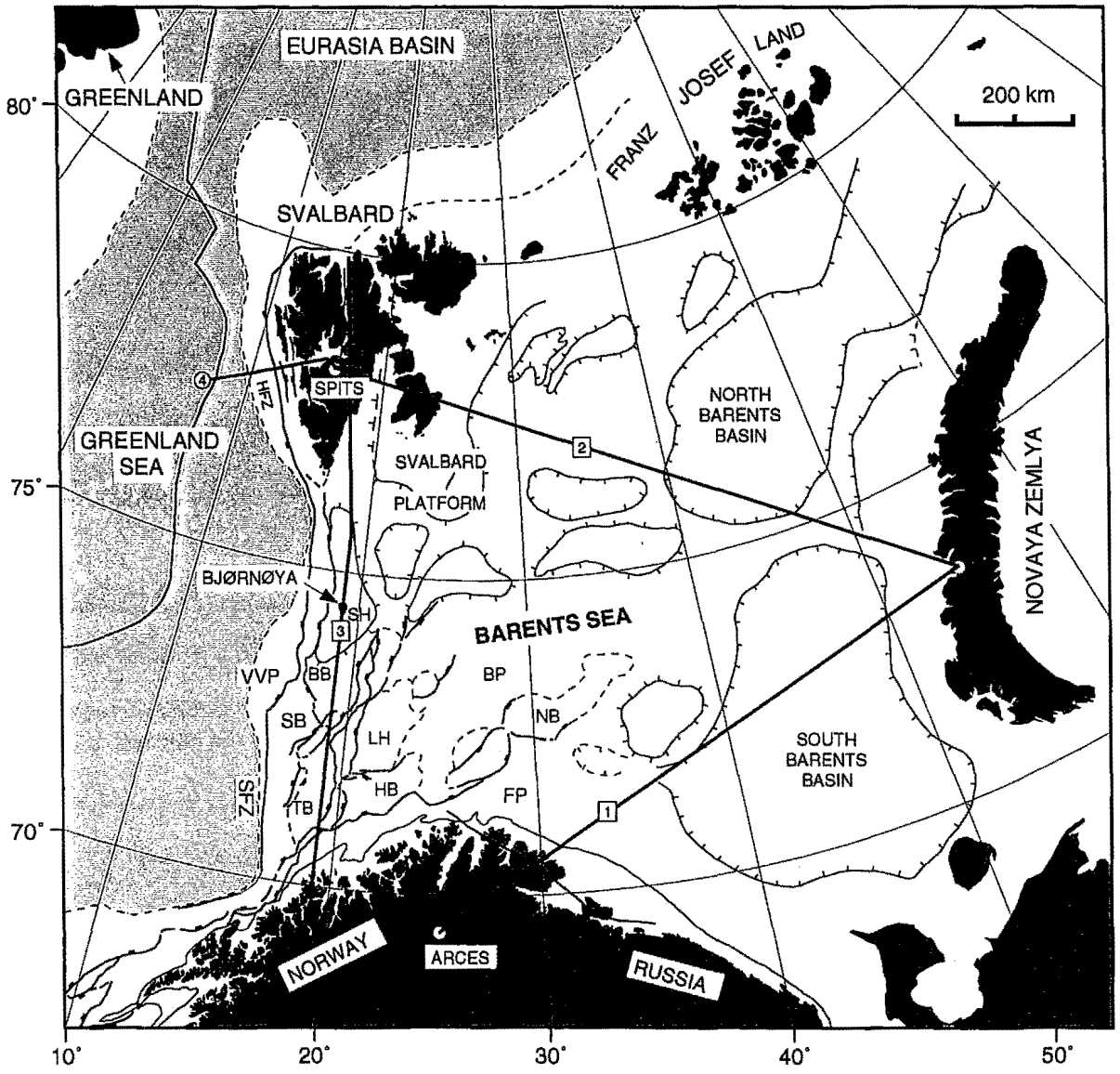

Figure 6.4.1. Regional setting - main geological provinces and structural elements in the Barents Sea and surrounding areas. Location of crustal transects and the seismic arrays SPITS and ARCES. BB = Bjørnøya Basin, BP = Bjarmeland Platform, FP = Finnmark Platform, HB = Hammerfest Basin, HFZ = Hornsund Fault Zone, LH = Loppa High, NB = Nordkapp Basin, SFZ = Senja Fracture Zone, SB = Sørvestnaget Basin, SH = Stappen High, TB = Tromsø Basin, VVP = Vestbakken Volcanic province (Faleide, 2000).

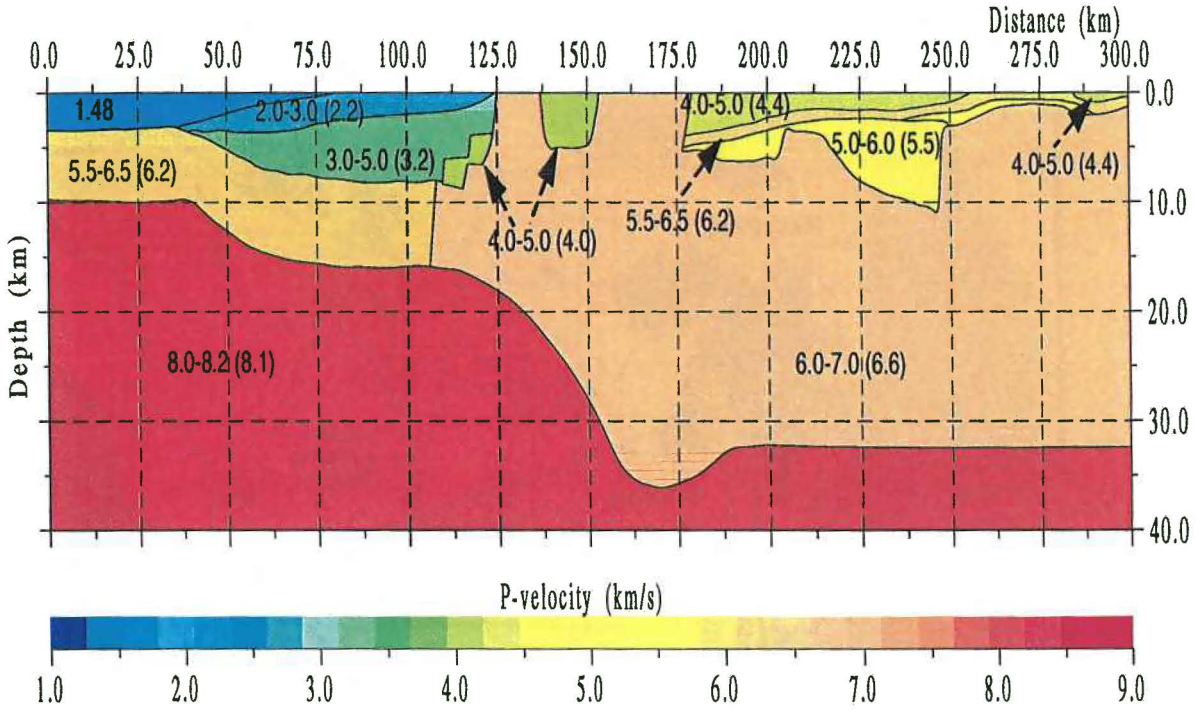

Figure 6.4.2. The crustal transect (Transect 4, Fig. 6.4.1) plotted together with the P-velocity range. A gradient has been assigned to all the layers based on the velocities in the brackets, and the gradient is varying with layer thickness. Vertical exaggeration (VE) = 3.

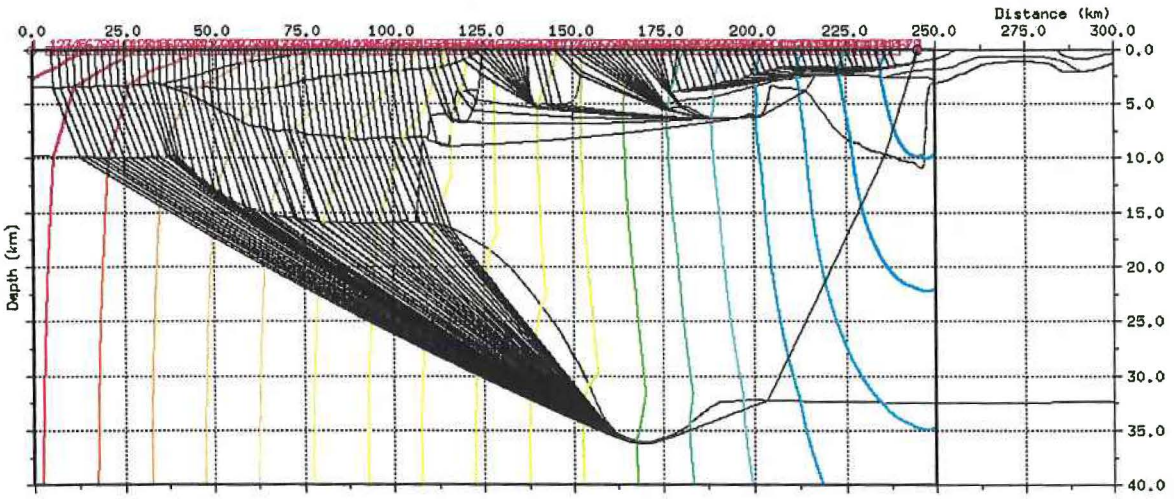

Figure 6.4.3. Ray paths from Transect 4 (Fig. 6.4.2) showing first arrivals (FD method). Wavefronts and ray paths are plotted together. VE = 3.

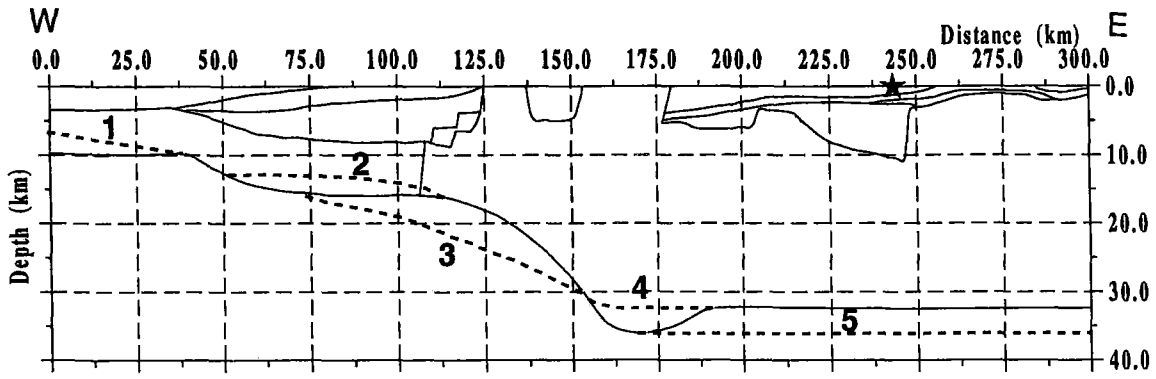

Figure 6.4.4. The different modifications of the Moho topography during the five sensitivity tests. The star indicates the location of the source.

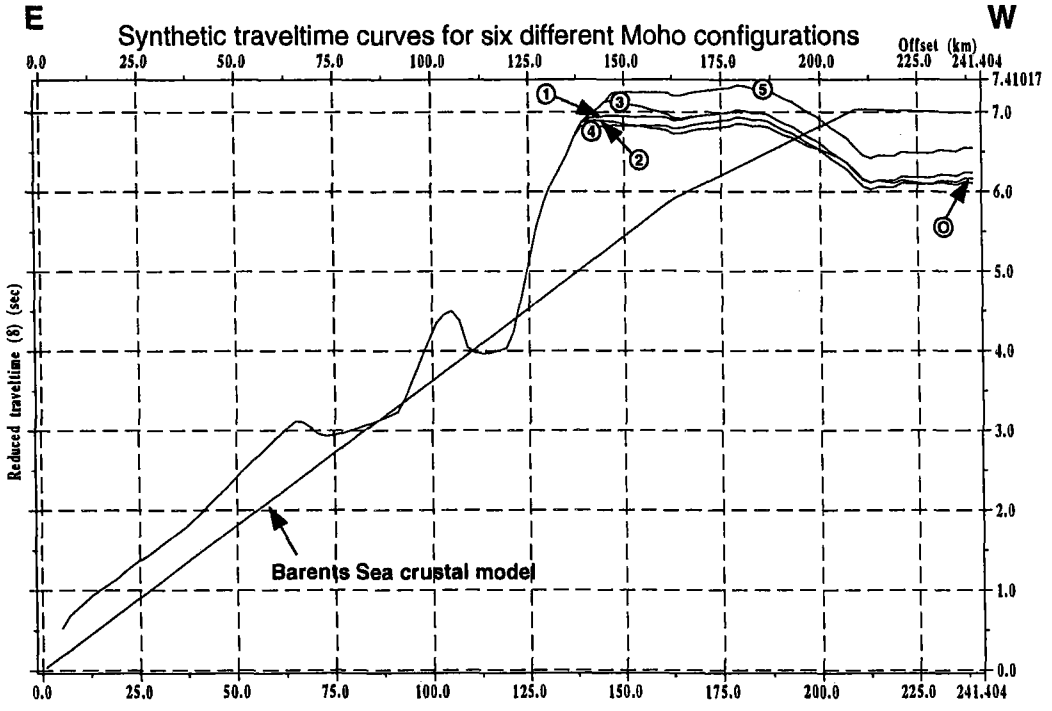

Figure 6.4.5. Synthetic travel time curves for the original Moho topography (O) and the five modifications (1 - 5), the numbers corresponds with Fig. 6.4.4. Transect 4 (Fig. 6.4.1) is shown from west to east, but the travel time curves are shown from east to west. The curves are deviating at most about 0.6 s, which indicate that the modelled details will hardly be resolvable with observed data. The travel time curve from the Barents Sea crustal model is shown for comparison.

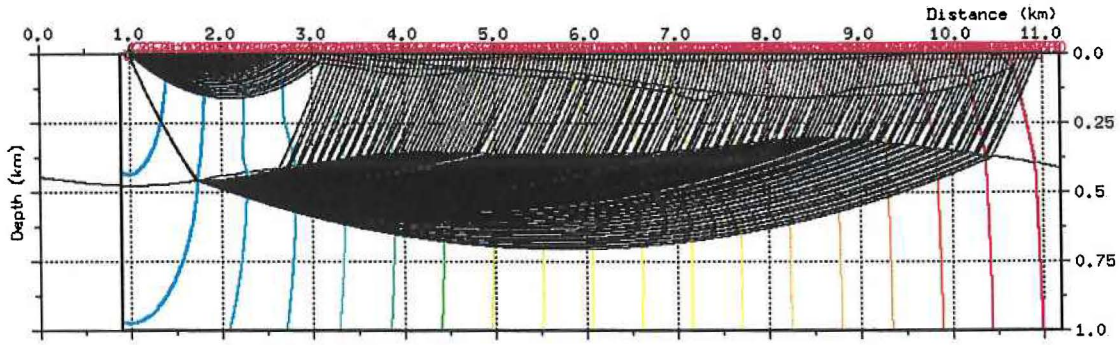

Figure 6.4.6. Ray paths for first arrivals (FD method) from ARCES to Novaya Zemlya (based on Transect 1 in Fig. 6.4.1). Source at the approximate location of ARCES. The model has been scaled down by the factor 0.01

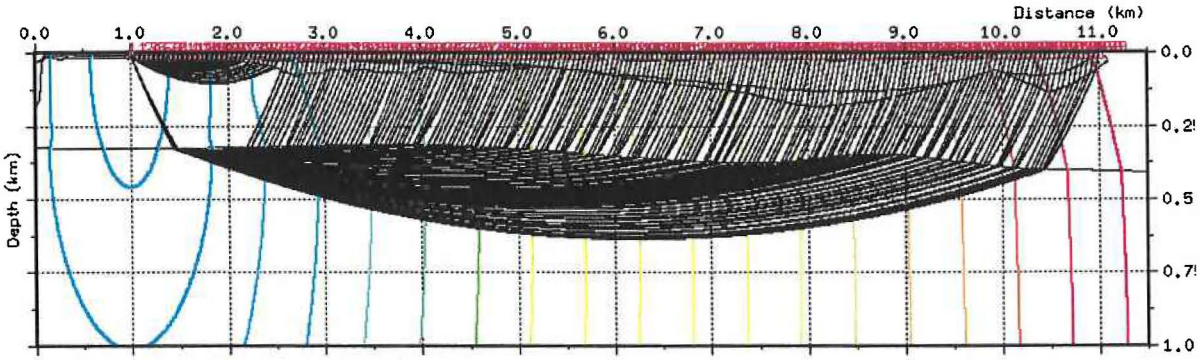

Figure 6.4.7. Ray paths for first arrivals (FD method) from SPITS to Novaya Zemlya (based on Transect 2 in Fig. 6.4.1). Source at the approximate location of SPITS. The model has been scaled down by the factor 0.01.

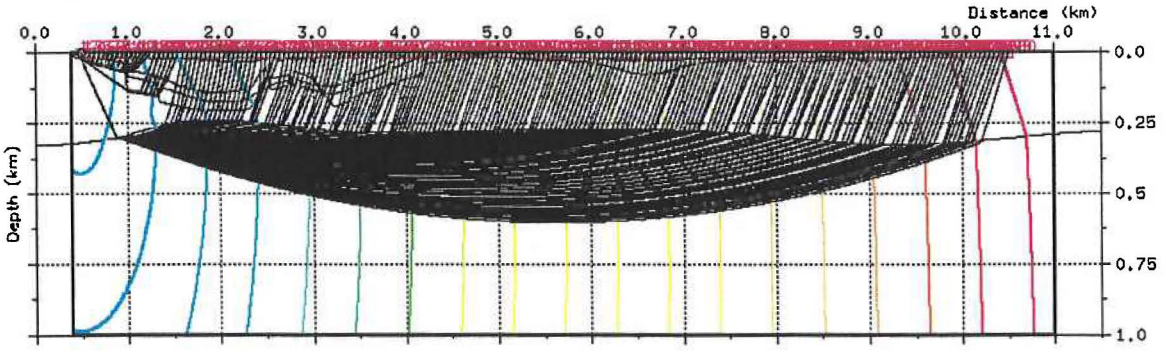

Figure 6.4.8. Ray paths for first arrivals (FD method) from northern Norway to SPITS (based on Transect 3 in Fig. 6.4.1). Source in northern Norway. The model has been scaled down by the factor 0.01.

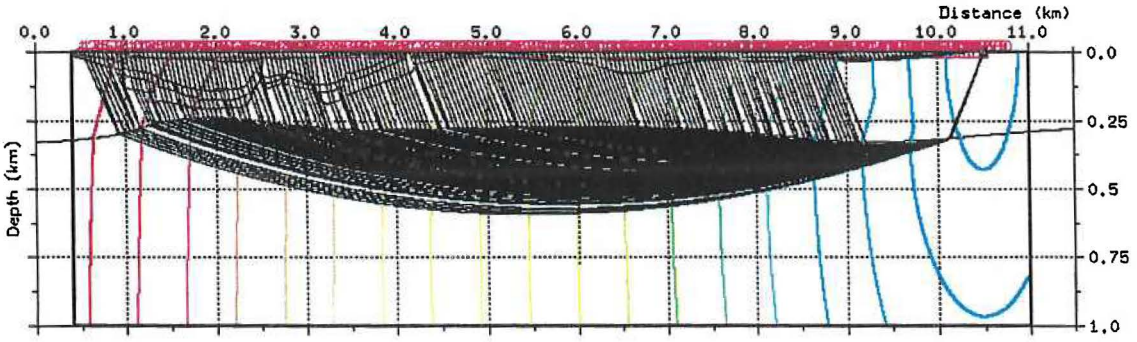

Figure 6.4.9. Ray paths for first arrivals (FD method) from SPITS to northern Norway (Transect 3, reversed survey, based on Transect 3 in Fig. 6.4.1). Source at the approximate location of SPITS. The model has been scaled down by the factor 0.01.

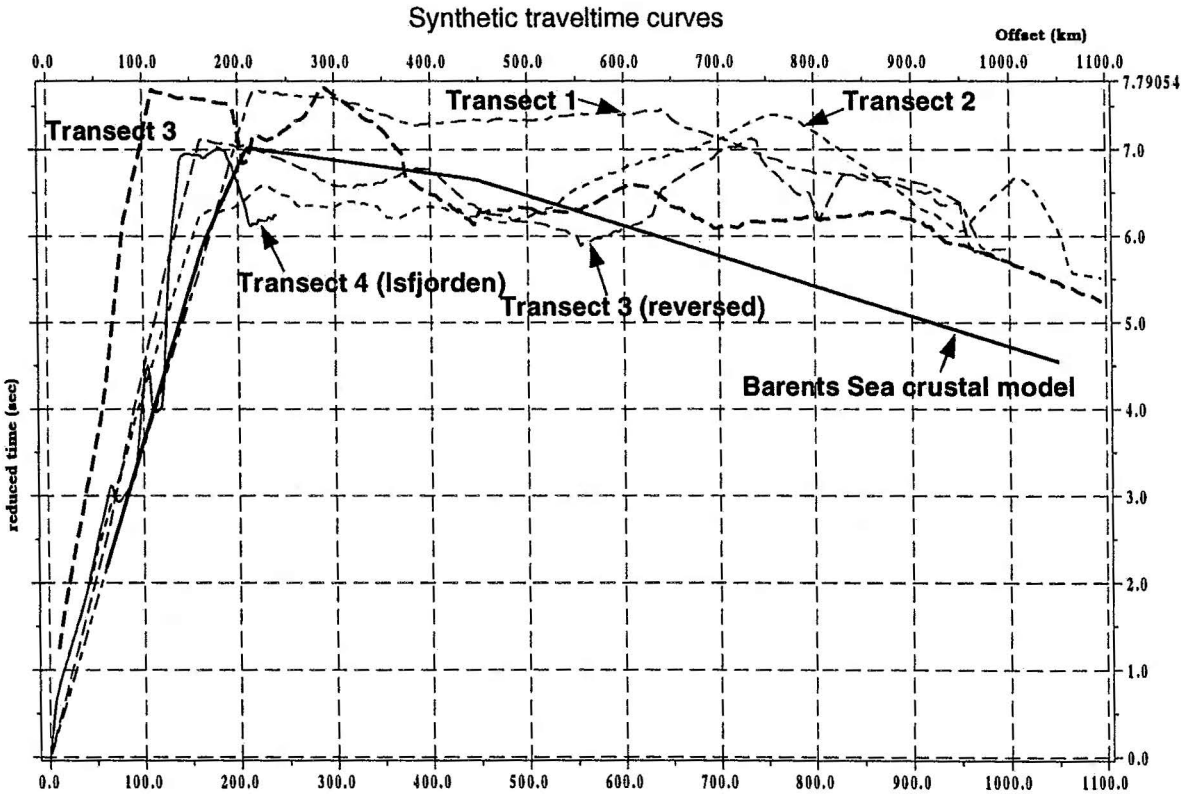

Figure 6.4.10. travel time curves from the five transects (six tests) including the Barents Sea crustal model and the Isfjord transect (Transect 4, Fig. 6.4.1). Barents Sea crustal model = thick/solid, Transect 1 = dashed/dotted, Transect 2 = dotted/thin, Transect 3 = dotted/thick, Transect 3 (reversed) = dashed/thin and Transect 4 (Isfjord) = solid/thin. Reduction velocity = 8 km/s. Note that these travel time curves are not scaled like the ray paths figures.